



Published in final edited form as:

Hepatology. 2008 June ; 47(6): 1983–1993. doi:10.1002/hep.22285.

Nitric Oxide Promotes Caspase-Independent Hepatic Stellate Cell Apoptosis Through the Generation of Reactive Oxygen Species

Daniel A. Langer¹, Amitava Das¹, David Semela¹, Ningling Kang-Decker¹, Helen Hendrickson¹, Steven F. Bronk², Zvonimir S. Katusic³, Gregory J. Gores², and Vijay H. Shah¹

¹Gastrointestinal Research Unit and Fiterman Center for Digestive Disease, Mayo Clinic College of Medicine, Rochester, MN.

²Center for Basic Research in Digestive Diseases and Fiterman Center for Digestive Disease, Division of Gastroenterology and Hepatology, Mayo Clinic College of Medicine, Rochester, MN.

³Department of Anesthesiology and Molecular Pharmacology and Experimental Therapeutics, Mayo Clinic College of Medicine, Rochester, MN.

Abstract

Hepatic stellate cells (HSCs) contribute to portal hypertension through multiple mechanisms that include collagen deposition, vasoconstriction, and regulation of sinusoidal structure. Under normal physiologic conditions, endothelial nitric oxide (NO) synthase–derived NO exerts paracrine effects on HSCs; however, in cirrhosis, NO generation is impaired in association with concomitant HSC activation and changes in sinusoidal structure, events that contribute significantly to the development of portal hypertension. These concepts, in combination with recent evidence that induction of HSC-selective apoptosis may represent a useful target for treatment of chronic liver disease, led us to examine if NO may further limit HSC function through apoptosis. Indeed, both NO donors and endothelial NO synthase overexpression promoted HSC apoptotic pathways. HSC death conferred by NO occurred through mitochondrial membrane depolarization and through a caspase-independent pathway. Furthermore, NO-induced apoptosis of HSC did not occur through the canonical pathways of soluble guanylate cyclase or protein nitration, but rather through the generation of superoxide and hydroxyl radical intermediates. Lastly, HSC isolated from rats after bile duct ligation were more susceptible to NO-induced apoptosis. These data indicate that NO promotes HSC apoptosis through a signaling mechanism that involves mitochondria, is mediated by reactive oxygen species, and occurs independent of caspase activation.

Conclusion—We postulate that NO-dependent apoptosis of HSCs may maintain sinusoidal homeostasis, and may represent an additional beneficial effect of NO donors for therapy of portal hypertension.

Hepatic stellate cells (HSCs) contribute to portal hypertension through multiple mechanisms that include collagen deposition, vasoconstriction, and regulation of sinusoidal structure.¹ In this regard, there is active investigation into mediators that can selectively promote HSC apoptosis, because they may have therapeutic use in portal hypertension.²

Under normal physiologic conditions, nitric oxide (NO) is generated constitutively from sinusoidal endothelial cell-derived endothelial NO synthase (eNOS), which in turn exerts

Address reprint requests to: Vijay Shah, GI Research Unit, Guggenheim 10, Mayo Clinic, 200 First Street SW, Rochester, MN55905. E-mail: shah.vijay@mayo.edu; fax: 507-255-6318.

Potential conflict of interest: Nothing to report.

paracrine effects on adjacent HSCs, culminating in the inhibition of vasoconstriction, proliferation, and migration.^{3–6} However, in cirrhosis, eNOS-derived NO generation is impaired in association with concomitant HSC activation and changes in sinusoidal structure,⁷ events that contribute significantly to the development of portal hypertension.^{1,8}

The most characterized NO signaling pathway occurs through the canonical protein kinase G pathway via activation of soluble guanylate cyclase.⁸ However, NO can also signal through complementary guanylate cyclase-independent pathways.^{9,10} These include tyrosine nitration and cysteine nitrosylation, which are protein modifications with wide-ranging effects. Finally, NO also affects the overall cellular redox potential by contributing to the formation of reactive nitrogen and oxygen species in the form of nitrosative stress and oxidative stress, respectively. These reactive intermediates also regulate cellular responses, especially apoptotic signaling.¹¹

Apoptosis is generally initiated by death receptor activation (extrinsic pathway) or intracellular stress (intrinsic pathway).¹² Either pathway may culminate in permeabilization of the outer membrane of mitochondria with resultant extrusion of mitochondrial proteins into cytoplasm. Classically, apoptosis is associated with activation of caspase proteases¹³; activation of the effector caspases 3 and 7 ultimately promotes chromatin condensation, cell fragmentation, and apoptotic body formation. More recently, a mitochondrial-dependent, apoptosis-like cell death that occurs independent of caspases has also been described.¹⁴

NO may reveal dichotomous effects on cell survival/death. For example, NO can directly impair apoptotic pathways through nitrosylation of caspases that results in their inactivation.^{15,16} However, NO can also contribute to apoptosis via nitrosylation or nitration of key signaling molecules or via impairment of mitochondrial respiratory chain electron transfer.¹⁷ Ultimately, multiple factors contribute to the determination of how NO affects cell survival, including cell type, redox microenvironment, and the balance of other proapoptotic versus antiapoptotic factors, and this paradigm has not been previously explored in the context of HSCs.¹¹

Given the negative regulatory properties of NO on HSC migration, contraction and proliferation, we tested the hypothesis that NO may limit HSC mass by promoting HSC apoptosis. Our data show that NO promotes HSC apoptosis through a signaling mechanism that involves mitochondria, is mediated by reactive oxygen species, and is independent of caspase activation. We postulate that NO-dependent apoptosis of HSCs may be a mechanism that maintains sinusoidal homeostasis and may be disrupted in the context of cirrhosis and portal hypertension. Furthermore, these studies predict that HSC apoptosis may represent an additional beneficial effect of NO donors for therapy of portal hypertension.

Materials and Methods

Reagents

Pharmacologic compounds used in this study included: cycloheximide (3 µg/mL), tumor necrosis factor- α (30 ng/mL; R&D Biosystems), 5,10,15,20-tetrakis(*N*-methyl-*r'*-pyridyl)porphinato iron (III) chloride (FeTMPyP; 100 µM), 1H-[1,2,4]oxadiazolo[4,3-*a*]quinoxalin-1-one (ODQ; 100 µM), 8-Bromo-cGMP (8-Br-cGMP; 100 µM; Calbiochem), tumor necrosis factor-related apoptosis-inducing ligand (TRAIL; 10 ng/mL), sodium nitroprusside (SNP; various doses), *S*-nitroso-*N*-acetylpenicillamine (SNAP), diethylamine NONOate (DEAN), diethylenetriamine NONOate (DETA), buthionine sulfoximine (BSO; 200 µM), uric acid (1 mM), deferoxamine (5–500 µM), dimethylthiourea (50 µM), mannitol (50 µM; Sigma), and compound 1799 (a generous gift from P. G. Heytden, E. I. du Pont, Bloomington, DE).¹⁸

Cell Isolation and Culture

All animal experiments were performed in accordance with and approved by the Mayo Clinic Institutional Animal Care and Use Committee. Primary rat HSCs were isolated from male Sprague-Dawley rats as described.³ Briefly, livers were perfusion digested with collagenase and pronase. Parenchymal and nonparenchymal cell fractions were separated via centrifugation. HSCs were purified via density-gradient centrifugation with 15.6% and 8.2% Accudenz gradient layers. The gradient was then centrifuged at 20,000 rpm for 25 minutes at 20°C. The band located above the 8.2% Accudenz layer was retrieved, and cells were resuspended in culture medium and plated on collagen-coated plastic culture dishes. Cell purity was verified to be approximately 95% with α -smooth muscle actin immunofluorescence. Rat HSCs were further cultured in plastic culture dishes using Dulbecco's minimal essential medium supplemented with 10% fetal bovine serum, 1% penicillin, and 1% streptomycin. Rat HSCs were used in experiments up to passage 2. Activation of the TRAIL pathway in rat HSCs was achieved through incubation of rat HSCs with TRAIL ligand (10 ng/mL) plus a low dose of cycloheximide (3 μ g/mL).

In some experiments, primary rat HSCs were isolated from bile duct–ligated (BDL) or sham-operated rats as controls 4 weeks after surgery. The technique of BDL has been described previously.¹⁹ Briefly, male Sprague-Dawley rats were anesthetized with sodium pentobarbital (50 mg/kg) and a small midline laparotomy performed under aseptic conditions. The common bile duct was localized and ligated both distally and proximally, followed by transection of the common bile duct between the ligatures. For sham controls, the common bile duct was exposed but not ligated or transected. The incision was closed in 2 layers.

Some experiments that required high efficiency transductions were performed in the human HSC line LX2, provided as a generous gift from Scott Friedman.²⁰ Cells were cultured in Dulbecco's minimal essential medium supplemented with 10% fetal bovine serum, 1% penicillin, and 1% streptomycin.

Primary rat hepatocytes were obtained from Cambrex Bioscience and cultured in media recommended by the vendor (Hepatocyte Basal Medium). Hepatocytes were used at passage 0.

Viral Transduction

Human LX2 HSCs were adenovirally transduced to overexpress endothelial nitric oxide synthase (eNOS) or green fluorescent protein control as described.³ Vectors were transduced into LX2 at a multiplicity of infection of 25, which achieved approximately 90% transduction efficiency with minimal toxicity. Activation of TRAIL pathway in LX2 was achieved through incubation of LX2 cells with TRAIL ligand (10 ng/mL).

Morphologic Quantitation of Apoptosis

To quantitate apoptosis in response to various culture conditions, characteristic apoptotic nuclei were counted as described.²¹ Briefly, 2.5×10^3 HSCs were plated in each well of 12-well plates and allowed to attach overnight. The density of 2.5×10^3 HSCs per well was determined to be the optimum value for studying cells in a logarithmic growth phase and optimizing uniform and accurate counting of apoptotic cells. Furthermore, in more confluent conditions, cells were more resistant to apoptotic stimuli. The following day, cells were washed and new media were added with various reagents as discussed in Results. At the time of harvest, 4',6-diamidino-2-phenylindole (DAPI; 5 μ g/mL) was added to culture media and cells counted (approximately 300 per well with triplicate wells used in each experimental group and each experiment repeated a minimum of three separate times) with characteristic DAPI stained

nuclei being defined as positive for apoptosis. Data were expressed as the percentage of cells that showed morphologic changes of apoptosis.

Proliferation Assay

The relative proliferation rates of rat HSCs were determined via MTS assay using 96-well plates as described.⁶

Griess Assay

To determine NO donor-derived generation and NO generation from cells in response to eNOS transduction, Griess assay was performed from cell culture supernatants as described.³

Measurement of Caspase Activity

Caspase activity of effector caspases 3 and 7 was determined using the APO-one assay kit (Promega). Cell lysates were analyzed for conversion of Z-DEVD-rhodamine 110 to fluorescent product, which was detected via fluorescent microplate reader.

Flow Cytometry

To further verify the apoptotic phenotype, cell cultures were also analyzed for annexin-V positivity. Annexin-V immuno-cytofluorescence was detected with flow cytometry and immuno-cytofluorescence according to the manufacturer's instructions (Roche Applied Sciences). Briefly, HSCs were collected after various treatment regimens and centrifuged. The cell pellet was washed in phosphate-buffered saline and centrifuged again. The pellet was resuspended in annexin-V according to the manufacturer's protocol (Roche). Cells were analyzed on a Becton-Dickinson flow cytometer, and the data were analyzed with WinMDI software.

Western Blot Analysis

HSCs were isolated after treatment and cells were homogenized in lysis buffer consisting of 50 mM Tris-HCl, 0.1 mM ethylene glycol tetraacetic acid, 0.1 mM ethylene diamine tetraacetic acid, 1% (vol/vol) NP-40, 0.1% deoxycholic acid (pH 7.5) with the addition of protease inhibitor cocktail (Roche). Protein quantitation was determined via Lowry assay. Equal quantities of protein were separated via sodium dodecyl sulfate–polyacrylamide gel electrophoresis on 7.5% to 15% polyacrylamide gels followed by electroblotting to PVDF membranes.⁴ Membranes were washed in Tris-buffered saline with 0.1% Tween and blocked with 5% milk. Primary antibodies were incubated for 1 hour at room temperature or overnight at 4°C. Primary antibodies included caspase 3 (Cell Signaling), β -actin (Sigma), and PARP-1 (Santa Cruz Biotechnology). Membranes were incubated with appropriate secondary antibody and detection was performed via enhanced chemiluminescence (Amersham).

Mitochondrial Membrane Potential Assay

HSCs were cultured on glass-bottom plates (MatTek) and treated with reagents for 18 hours. Mitochondrial membrane potential was determined as described.²¹ Briefly, cellular fluorescence was quantitated after loading with mitochondrial-specific fluorophore tetramethylrhodamine methylester (250 nM) and again after complete mitochondrial depolarization with mitochondrial uncoupling compound 1799 (25 μ M). The difference in fluorescence was expressed as the mitochondrial membrane potential. A minimum of 15 randomly selected cells were analyzed per condition from multiple microscopic fields and the experiment was replicated three times.

Fluorescence Microscopy

HSCs were cultured on glass slides and exposed to experimental conditions. Cells were fixed with 4% paraformaldehyde and permeabilized with 0.1% Triton-X for 5 minutes. Blocking was performed with 3% milk and 10% goat serum. Primary antibody (3-nitrotyrosine, Cayman) was incubated at room temperature for 2 hours. Alexafluor 488-tagged secondary antibody was incubated for 2 hours at room temperature. Cells were analyzed with fluorescent microscopy using a Zeiss LSM confocal microscope.

Peroxynitrite Quantitation

Primary rat HSCs were plated in 96-well plates at a density of 1000 cells per well and allowed to attach overnight. Cells were washed and loaded with 2 μ M fluorophore dihydrorhodamine-123 (DHR123) in serum-free media for 30 minutes. When exposed to peroxynitrite, intracellular DHR123 will become oxidized yielding a fluorescent product and is sensitive and selective for peroxynitrite.^{22,23} Cells were washed and exposed to uric acid 1 mM or control for 30 minutes. Following an additional wash, cells were exposed to the indicated experimental conditions for 3 hours. Cells were washed with PBS and fluorescence determined with a Molecular Devices Spectramax Gemini XS fluorescent microplate reader using 488 nm excitation and 530 nm emission wavelengths. Some experiments were also performed after exposure to experimental conditions for 18 hours.

Statistical Analysis

Experiments were performed in triplicate with a minimum of three independent experiments performed from different HSC preparations. Data are depicted as the mean \pm standard error of the mean. Comparisons were performed via Student *t* test or one-way analysis of variance when comparing more than two sample groups, with statistical significance set at $P < 0.05$.

Results

NO Promotes HSC Apoptosis

To first test the concept that NO may promote HSC apoptosis, primary rat HSCs were exposed to the prototypical NO donor SNP at varying concentrations and durations, and apoptosis was measured via morphologic criteria with DAPI staining by fluorescent microscopy as well as annexin-V positivity (Fig. 1A,B). The magnitude of apoptosis was both concentration and time-dependent, with up to 40% of cells evidencing morphologic features of apoptosis at 18 hours at a concentration of 250 μ M (Fig. 1C,D). Annexin-V staining in response to SNP correlated with morphologic measurements of apoptosis (SNP 50 μ M after 18 hours; 14.3% with annexin positivity and 17.5% with morphologic features of apoptosis; Fig. 1B,C). To avoid nonspecific actions of SNP, all subsequent experiments were performed using an SNP concentration of 50 μ M or lower. This dose is consistent with the literature and generated a concentration of 5.0 μ M of nitrite after 4 hours as measured by Griess assay, a level that is comparable to prior studies that have examined NO generation in response to NO donors in more detail.^{24–26} To confirm that the effect of SNP was not increasing apoptosis by reducing cell proliferation, an MTS assay was used to measure HSC proliferation in response to SNP. At doses up to 50 μ M SNP, there was no significant effect of SNP on HSC proliferation rate [SNP (50 μ M), 147% \pm 20%, vehicle, 146% \pm 2%, at 24 hours; $n=3$, P value not significant]. SNP-mediated apoptosis of HSCs was cell-type selective, because hepatocytes were resistant to increased apoptosis in response to SNP compared with HSCs (Fig. 1E). Because SNP may also have effects on cells independent of the NO moiety owing to its CN group, we used the analogous compound iron (III) hexacyanide [Fe(III)(CN)₆], which does not contain the NO moiety to confirm NO-dependent specificity of effect. At up to 10-fold higher concentrations, iron (III) hexacyanide did not result in any appreciable apoptosis. Furthermore, two other NO donors that do not

contain the Fe or CN moiety, SNAP and DEAN, also increased HSC apoptosis rate, albeit at higher concentrations [DEAN (1 mM), 24.8% ± 0.4; SNAP (1 mM), 32.5% ± 8.8; vehicle, 7.5% ± 0.7]. A third NO donor, DETA, was also tested, which, at a concentration of 1 mM, is thought to generate an NO flux of approximately 2.6 μM, a level akin to that observed in response to pathological conditions in vivo.^{27,28} DETA also increased HSC apoptosis in a concentration-dependent manner with up to 44% apoptosis after exposure to 1000 μM [vehicle, 5.2% ± 1.2; DETA (50 μM), 25.7% ± 0.9; DETA (500 μM), 32.4% ± 2.4; DETA (1000 μM), 43.9% ± 6.6; n = 3, P < 0.01 all values compared with control]. We chose to use SNP for subsequent experiments because of the more potent effects of this compound as well as the greater clinical applicability of SNP, which is a compound that is approved for human use. As another complementary approach to establish the NO dependency of the NO donor studies, cells were adenovirally transduced to overexpress eNOS or green fluorescent protein control to determine whether enhanced endogenous NO favors apoptotic pathways in HSCs (Fig. 1F). For this experiment, we used human LX2 cells, which are more amenable to high level transduction than primary HSCs. Although eNOS overexpression by itself did not increase basal apoptosis, eNOS overexpression significantly sensitized HSCs to apoptosis mediated by the prototypical HSC death receptor agonist TRAIL (Fig. 1F). This high-level adenoviral eNOS overexpression system resulted in a 10-fold increase in NO metabolite concentration in culture media after 4 hours compared with control cells.

NO Donor-Mediated Apoptosis Is Caused by Mitochondrial Dysfunction but Is Caspase-Independent

We next sought to probe the mechanism by which NO induces HSC apoptosis. Apoptotic pathways can lead to mitochondrial dysfunction characterized by mitochondrial membrane depolarization and permeabilization of the mitochondrial outer membrane.¹⁴ First, to determine whether HSCs undergoing SNP-mediated apoptosis develop mitochondrial dysfunction, we quantitated the mitochondrial membrane potential ($\Delta\Psi_m$; Fig. 2A). Under normal culture conditions, HSCs demonstrated a high resting $\Delta\Psi_m$. However, when exposed to SNP (50 μM), there was a large and significant decrease in $\Delta\Psi_m$ comparable to that observed in cells exposed to TRAIL pathway activation. Next, to determine the role of classical caspase-dependent apoptotic signaling, we examined the effects of the pancaspase inhibitors z-VAD-fmk and qVD-OPH on SNP-induced HSC apoptosis. Pancaspase inhibitors did not attenuate SNP-induced apoptosis in HSCs (Fig. 2B), although they did protect cells from apoptosis induced by the TRAIL pathway. To explore this further, we determined the activity of effector caspases via direct activity assay (caspases 3 and 7) and also via western blot analysis for cleaved caspase 3 from HSCs exposed to SNP (Fig. 2C and D). Although the TRAIL pathway increased effector caspase activity, there was no significant increase in effector caspase activity in HSCs exposed to SNP (Fig. 2C). Western blot and densitometry analysis for cleaved caspase 3 levels corroborated the caspase activity results and furthermore, PARP-1 cleavage, another marker of caspase-dependent apoptosis mirrored the changes observed in cleaved caspase 3 levels (Fig. 2D). In fact, cells exposed to TRAIL pathway activation and SNP displayed significant inhibition of caspase activity on both activity assay and western blot analysis compared with cells exposed to TRAIL alone (Fig. 2D). This finding is probably due to the ability of NO to nitrosylate the active site of caspase 3, thereby impairing its activity as shown previously.²⁹ Nonetheless, the combination of TRAIL pathway activation and SNP resulted in a 90% rate of apoptosis based on morphologic criteria in response to both compounds together (data not shown). These complementary observations highlight the distinct caspase-dependent apoptosis conferred by TRAIL pathway activation as opposed to the caspase-independent apoptosis conferred by SNP and the additive effects of both pathways in combination.

SNP-Mediated Apoptosis Is Independent of Soluble Guanylate Cyclase and Protein Nitration but Is Dependent on Superoxide and Hydroxyl Radical Generation

We next explored which specific NO signaling pathways were responsible for SNP-induced apoptosis of HSCs. First, to evaluate the canonical soluble guanylate cyclase pathway, we used the degradation-resistant protein kinase G agonist, 8-Br-cGMP, and the guanylate cyclase antagonist, ODQ. In pilot experiments, both compounds demonstrated specific biological activity at a concentration of 100 μM as described.³ 8-Br-cGMP did not mimic the apoptotic phenotype of SNP, nor did ODQ inhibit SNP-induced apoptosis (Fig. 3A), suggesting that SNP induces HSC apoptosis through a guanylate cyclase/protein kinase G-independent signaling pathway.

NO interaction with superoxide anion can generate peroxynitrite, which in turn promotes signaling through tyrosine nitration-dependent regulation of target proteins.³⁰ However, SNP did not generate peroxynitrite in HSCs as evaluated with the peroxynitrite-specific fluorescent probe DHR123 at neither 3 hours nor after 18 hours of incubation with SNP^{22,23} (Fig. 3B shows 3-hour data) nor via immunocytochemistry using a 3-nitrotyrosine antibody (Fig. 3C). In these experiments, we used SIN-1, a known generator of peroxynitrite, as a positive control,^{30,31} and uric acid as a scavenger of peroxynitrite generation.³² Interestingly, the peroxynitrite generator, SIN-1, unlike SNP, did not cause HSC apoptosis (data not shown), further supporting the role of a peroxynitrite-independent mechanism of SNP.

NO can also activate redox pathways, which generate oxidative stress mediators. To explore the role of these potential stress mediators in the process of SNP-induced HSC apoptosis, we used complementary mechanism-based antioxidants, including the superoxide dismutase (SOD) mimetic, FeTMPyP, the hydroxyl ion scavenger, deferoxamine, and the peroxynitrite scavenger, uric acid.^{33–36} Although FeTMPyP significantly blunted SNP-mediated apoptosis by approximately 40% (Fig. 4A), an even more prominent effect was observed with hydroxyl radical scavenger deferoxamine, which significantly impaired SNP-mediated apoptosis in a concentration-dependent manner (Fig. 4B) and also impaired apoptosis induced by a different NO donor, DEAN (Fig. 4C). These observations were also confirmed by using two additional, mechanistically distinct hydroxyl radical scavengers, dimethylurea and mannitol (Fig. 4D).^{33–35} Conversely, uric acid, a peroxynitrite scavenger, did not protect HSCs from SNP-mediated apoptosis (Fig. 4E), consistent with results from Fig. 3. Although uric acid has been implicated in hydroxyl radical scavenging as well, these experiments in total, conducted with three distinct and well characterized hydroxyl radical scavengers, suggest an important role for oxidative stress, especially hydroxyl radicals and to a lesser extent, superoxide anion, in the process of NO-mediated apoptosis of HSCs.

Enhanced Oxidative Stress Exacerbates SNP-Mediated Apoptosis

Given the importance of oxidative stress in the process of SNP-mediated apoptosis of HSCs, we postulated that this pathway may be accentuated in conditions of elevated oxidative stress. To pursue this concept further, HSCs were treated with the glutathione-depleting compound BSO,³⁷ prior to exposure to SNP. Indeed, BSO increased SNP-mediated apoptosis in a synergistic manner (Fig. 5A). Lastly, because oxidative stress is enhanced in the cirrhotic microenvironment,^{38,39} we determined whether HSCs isolated from rats after BDL were more sensitive to SNP-mediated apoptosis. Indeed, HSCs isolated from BDL rats were significantly more sensitive to apoptosis induced by SNP compared with HSCs isolated from sham [Fig. 5B; despite similar rates of proliferation between sham and BDL HSCs (sham, $182.2\% \pm 3.1$, and BDL, $182.9\% \pm 1.6\%$, at 24 hours; $n = 3$, P value not significant)], suggesting *in vivo* relevance to the process of SNP-induced HSC apoptosis.

Discussion

NO negatively regulates diverse HSC functions that lead to the HSC “activation” phenotype of portal hypertension, including HSC proliferation, migration, and contraction.^{3–6} In this study, we demonstrated that NO also has the capacity to promote HSC apoptosis, thereby providing an additional mechanism by which NO maintains a check on HSC activation in portal hypertension. Interestingly, extensive experimental data indicates that oxidative stress contributes to the development of fibrosis and vascular remodeling in portal hypertension.^{40–42} However, a complementary line of work, including the present study, indicates that oxidative stress can also promote HSC apoptosis,^{43,44} thus highlighting the paradoxical effects of oxidative stress in liver pathobiology. Indeed, in the present studies, when HSCs were preincubated with BSO, there was significantly increased sensitivity to NO donor-mediated apoptosis.³⁷ Furthermore, HSCs isolated from rats after BDL, which are exposed to increased oxidative stress *in vivo*, also displayed an increased sensitivity to NO donor-mediated apoptosis.⁴⁵ These data suggest that increased oxidative stress, such as that observed in the cirrhotic microenvironment, may predispose HSCs to NO-dependent apoptosis. Conversely, impaired NO generation in cirrhotic liver may allow for increased HSC mass.

NO may have dichotomous effects on cell apoptosis depending on cell type, microenvironment, and other unrecognized factors.^{11,46,47} For example, NO promotes endothelial cell growth and resistance to apoptosis.⁴⁶ Alternatively, in other cell types, NO displays inhibitory and proapoptotic characteristics.¹¹ These dichotomous effects of NO on apoptosis may relate in part to divergent mechanisms by which NO induces oxidative stress as opposed to NO actions as an antioxidant. For example, in support of the latter concept, NO binds superoxide, thereby quenching potential ROS signaling. Yet in reacting with superoxide, NO may promote the formation of a more potent oxidant, peroxynitrite. Furthermore, recent work from Moncada’s group demonstrates that NO also impairs the respiratory electron transport chain by inhibition of cytochrome oxidase, thereby resulting in the formation of superoxide: a process referred to as metabolic hypoxia.^{17,48} In our study, the apoptotic actions of NO associated with changes in mitochondrial membrane potential, and partial inhibition of this process by SOD mimetics support the concept that NO stimulates generation of mitochondrial oxidative stress in HSCs through this process. Furthermore, recent studies have indicated that lysosomal stress may also contribute to caspase-independent cell death. Indeed, the protective effect of deferoxamine observed in this study may be related to suppression of the Fenton reaction within lysosomes whereby hydroxyl radical generation is impaired by the chelation of lysosomal iron.^{37,49–51} Alternatively, hydroxyl radicals may be then “scavenged” by deferoxamine. Although the precise mechanism of action of deferoxamine remains uncertain, the ability of two complementary hydroxyl radical scavengers not implicated in disruption of the Fenton reaction (dimethylurea and mannitol) to impair SNP-induced apoptosis clearly implicates hydroxyl radicals in the process of NO-induced apoptosis of HSCs. These complementary effects of SOD mimetic agents and hydroxyl radical scavengers provide evidence for lysosomal synergy with mitochondria in the process of SNP-dependent cell death signaling in HSCs.

Although apoptotic cell death has traditionally been associated with caspase activation, recent work has highlighted a process whereby cell death occurs in association with characteristic morphologic features of apoptosis yet is not attenuated by inhibitors of caspases.¹⁴ Although not fully understood, current concepts suggest that this occurs through increased mitochondrial permeability that leads to extrusion and nuclear translocation of mitochondrial proteins. This in turn, leads to ROS generation and chromatin condensation independent of effector caspase activation.^{14,52,53} Thus, regulation of mitochondrial outer membrane permeability appears to be a critical and lethal step in caspase-independent apoptotic cell death. Indeed, in the present study, SNP significantly reduced mitochondrial membrane potential in HSCs.

In vivo studies support the concept that NO delivery to the hepatic vasculature may improve portal hypertension through complementary mechanisms. For example, the liver-specific NO donors NCX-1000 and V-PYRRO/NO improve portal hemodynamics in complementary models of portal hypertension largely through vasoregulatory effects of NO.^{54–56} The present study identifies new vasodilation-independent, HSC apoptosis-dependent pathways by which NO supplementation in chronic liver disease may be beneficial. Furthermore, HSCs displayed greater sensitivity to NO-mediated apoptosis compared with hepatocytes, a point that may be important when considering the therapeutic potential of this approach. Interestingly, in the present study, SNP was a more potent apoptotic stimulus of HSCs than other NO donors that were evaluated and also more potent compared with NO derived from eNOS. This may relate to the rapid NO burst characteristics of SNP compared with other NO donors.^{57,58} Indeed, the NO release kinetics of SNP account for its use as a therapeutic agent in humans with malignant hypertension and its potency for HSC-selective ROS generation provides a potentially translational clinical correlate to our work. Nonetheless, lack of liver selectivity continues to be a hurdle with the use of traditional NO donors in portal hypertension owing to systemic side effects. As work continues toward developing liver-selective compounds, the present study suggests that certain NO-donating moieties may be preferable to others depending on their specific NO release kinetics and the specific NO-dependent biological outcome that is desired (HSC apoptosis, vasodilation, or others). For example, although DEAN is not a potent stimulus for HSC apoptosis, it nicely promotes HSC relaxation, another important biological endpoint that retards portal hypertension.³ The present study suggests that the HSC selectivity of NO-mediated apoptosis may provide a process for normalization of HSC mass and sinusoidal structure in cirrhosis and portal hypertension, providing additional mechanisms by which NO promotes hepatic vascular homeostasis.

Abbreviations

BDL, bile duct-ligated
 8-Br-cGMP, 8-Bromo-cGMP
 BSO, buthionine sulfoximine
 DAPI, 4',6-diamidino-2-phenylindole
 DEAN, diethylamine NONOate
 DETA, diethylenetriamine NONOate
 DHR123, dihydrorhodamine-123
 eNOS, endothelial nitric oxide synthase
 FeTMPyP, 5,10,15,20-tetrakis(N-methyl-r'-pyridyl)porphyrinato iron (III) chloride
 HSC, hepatic stellate cell
 NO, nitric oxide
 ODQ, 1H-[1,2,4]oxadiazolo[4,3-a]quinoxalin-1-one
 SNAP, S-nitroso-N-acetylpenicillamine
 SNP, sodium nitroprusside
 SOD, superoxide dismutase
 TRAIL, tumor necrosis factor-related apoptosis-inducing ligand

Acknowledgements

Supported by National Institutes of Health (NIH) grants R01 DK059615-VS, R01 DK59388-VS, and R37 DK041876-GG. D. A. L. was supported by grant T32 DK07198-VS.

References

1. Langer DA, Shah VH. Nitric oxide and portal hypertension: interface of vasoreactivity and angiogenesis. *J Hepatol* 2006;44:209–216. [PubMed: 16297493]

2. Elsharkawy AM, Oakley F, Mann DA. The role and regulation of hepatic stellate cell apoptosis in reversal of liver fibrosis. *Apoptosis* 2005;10:927–939. [PubMed: 16151628]
3. Perri RE, Langer DA, Chatterjee S, Gibbons SJ, Gadgil J, Cao S, et al. Defects in cGMP-PKG pathway contribute to impaired NO-dependent responses in hepatic stellate cells upon activation. *Am J Physiol Gastrointest Liver Physiol* 2006;290:G535–G542. [PubMed: 16269521]
4. Shah V, Haddad FG, Garcia-Cardena G, Frangos JA, Mennone A, Groszmann RJ, et al. Liver sinusoidal endothelial cells are responsible for nitric oxide modulation of resistance in the hepatic sinusoids. *J Clin Invest* 1997;100:2923–2930. [PubMed: 9389760]
5. Failli P, De FR, Caligiuri A, Gentilini A, Romanelli RG, Marra F, et al. Nitrovasodilators inhibit platelet-derived growth factor-induced proliferation and migration of activated human hepatic stellate cells. *Gastroenterology* 2000;119:479–492. [PubMed: 10930383]
6. Lee JS, Decker N, Chatterjee S, Yao J, Friedman S, Shah V. Mechanisms of nitric oxide interplay with Rho GTPase family members in modulation of actin membrane dynamics in pericytes and fibroblasts. *Am J Pathol* 2005;166:1861–1870. [PubMed: 15920170]
7. Lee JS, Semela D, Iredale J, Shah VH. Sinusoidal remodeling and angiogenesis: a new function for the liver-specific pericyte? *Hepatology* 2007;45:817–825. [PubMed: 17326208]
8. Shah V. Cellular and molecular basis of portal hypertension. *Clin Liver Dis* 2001;5:629–644. [PubMed: 11565134]
9. Greenacre SA, Ischiropoulos H. Tyrosine nitration: localisation, quantification, consequences for protein function and signal transduction. *Free Radic Res* 2001;34:541–581. [PubMed: 11697033]
10. Stamler JS, Lamas S, Fang FC. Nitrosylation. the prototypic redox-based signaling mechanism. *Cell* 2001;106:675–683. [PubMed: 11572774]
11. Brune B. The intimate relation between nitric oxide and superoxide in apoptosis and cell survival. *Antioxid Redox Signal* 2005;7:497–507. [PubMed: 15706097]
12. Jin Z, El-Deiry WS. Overview of cell death signaling pathways. *Cancer Biol Ther* 2005;4:139–163. [PubMed: 15725726]
13. Hengartner MO. The biochemistry of apoptosis. *Nature* 2000;407:770–776. [PubMed: 11048727]
14. Kroemer G, Martin SJ. Caspase-independent cell death. *Nat Med* 2005;11:725–730. [PubMed: 16015365]
15. Benhar M, Stamler JS. A central role for S-nitrosylation in apoptosis. *Nat Cell Biol* 2005;7:645–646. [PubMed: 15990893]
16. Torok NJ, Higuchi H, Bronk S, Gores GJ. Nitric oxide inhibits apoptosis downstream of cytochrome C release by nitrosylating caspase 9. *Cancer Res* 2002;62:1648–1653. [PubMed: 11912135]
17. Moncada S, Erusalimsky JD. Does nitric oxide modulate mitochondrial energy generation and apoptosis? *Nat Rev Mol Cell Biol* 2002;3:214–220. [PubMed: 11994742]
18. Bronk SF, Gores GJ. Acidosis protects against lethal oxidative injury of liver sinusoidal endothelial cells. *Hepatology* 1991;14:150–157. [PubMed: 2066063]
19. Hendrickson H, Chatterjee S, Cao S, Morales Ruiz M, Sessa WC, Shah V. Influence of caveolin on constitutively activated recombinant eNOS: insights into eNOS dysfunction in BDL rat liver. *Am J Physiol Gastrointest Liver Physiol* 2003;285:G652–G660. [PubMed: 12829439]
20. Xu L, Hui AY, Albanis E, Arthur MJ, O’Byrne SM, Blaner WS, et al. Human hepatic stellate cell lines, LX-1 and LX-2: new tools for analysis of hepatic fibrosis. *Gut* 2005;54:142–151. [PubMed: 15591520]
21. Malhi H, Bronk SF, Werneburg NW, Gores GJ. Free fatty acids induce JNK-dependent hepatocyte lipoapoptosis. *J Biol Chem* 2006;281:12093–12101. [PubMed: 16505490]
22. Kooy NW, Royall JA, Ischiropoulos H, Beckman JS. Peroxynitrite-mediated oxidation of dihydrorhodamine 123. *Free Radic Biol Med* 1994;16:149–156. [PubMed: 8005510]
23. Crow JP. Dichlorodihydrofluorescein and dihydrorhodamine 123 are sensitive indicators of peroxynitrite in vitro: implications for intracellular measurement of reactive nitrogen and oxygen species. *Nitric Oxide* 1997;1:145–157. [PubMed: 9701053]
24. Smith JN, Dasgupta TP. Mechanisms of nitric oxide release from nitrovasodilators in aqueous solution: reaction of the nitroprusside ion ([Fe(CN)5NO]2-) with L-ascorbic acid. *J Inorg Biochem* 2001;87:165–173. [PubMed: 11730898]

25. Li MH, Jang JH, Surh YJ. Nitric oxide induces apoptosis via AP-1-driven upregulation of COX-2 in rat pheochromocytoma cells. *Free Radic Biol Med* 2005;39:890–899. [PubMed: 16140209]
26. Du C, Guan Q, Diao H, Yin Z, Jevnikar AM. Nitric oxide induces apoptosis in renal tubular epithelial cells through activation of caspase-8. *Am J Physiol Renal Physiol* 2006;290:F1044–F1054. [PubMed: 16352744]
27. Schmidt K, Desch W, Klatt P, Kukovetz WR, Mayer B. Release of nitric oxide from donors with known half-life: a mathematical model for calculating nitric oxide concentrations in aerobic solutions. *Naunyn Schmiedebergs Arch Pharmacol* 1997;355:457–462. [PubMed: 9109361]
28. DetaNONOate product insert. Cayman Chemical; 2007. Catalog no. 82120,
29. Mannick JB, Schonhoff C, Papeta N, Ghafourifar P, Szibor M, Fang K, et al. S-Nitrosylation of mitochondrial caspases. *J Cell Biol* 2001;154:1111–1116. [PubMed: 11551979]
30. Beckman JS, Koppenol WH. Nitric oxide, superoxide, and peroxynitrite: the good, the bad, and ugly. *Am J Physiol* 1996;271:C1424–C1437. [PubMed: 8944624]
31. Knepler JL Jr, Taher LN, Gupta MP, Patterson C, Pavalko F, Ober MD, et al. Peroxynitrite causes endothelial cell monolayer barrier dysfunction. *Am J Physiol Cell Physiol* 2001;281:C1064–C1075. [PubMed: 11502585]
32. Santos CX, Anjos EI, Augusto O. Uric acid oxidation by peroxynitrite: multiple reactions, free radical formation, and amplification of lipid oxidation. *Arch Biochem Biophys* 1999;372:285–294. [PubMed: 10600166]
33. Jiang M, Wei Q, Pabla N, Dong G, Wang CY, Yang T, Smith SB, et al. Effects of hydroxyl radical scavenging on cisplatin-induced p53 activation, tubular cell apoptosis and nephrotoxicity. *Biochem Pharmacol* 2007;73:1499–1510. [PubMed: 17291459]
34. Santos NA, Bezerra CS, Martins NM, Curti C, Bianchi ML, Santos AC. Hydroxyl radical scavenger ameliorates cisplatin-induced nephrotoxicity by preventing oxidative stress, redox state unbalance, impairment of energetic metabolism and apoptosis in rat kidney mitochondria. *Cancer Chemother Pharmacol* 2008;61:145–155. [PubMed: 17396264]
35. Yu Z, Persson HL, Eaton JW, Brunk UT. Intralysosomal iron: a major determinant of oxidant-induced cell death. *Free Radic Biol Med* 2003;34:1243–1252. [PubMed: 12726912]
36. Pryor WA, Houk KN, Foote CS, Fukuto JM, Ignarro LJ, Squadrito GL, et al. Free radical biology and medicine: it's a gas, man! *Am J Physiol Regul Integr Comp Physiol* 2006;291:R491–R511. [PubMed: 16627692]
37. Fruehauf JP, Zonis S, al-Bassam M, Kyshtoobayeva A, Dasgupta C, Milovanovic T, et al. Melanin content and downregulation of glutathione S-transferase contribute to the action of L-buthionine-S-sulfoximine on human melanoma. *Chem Biol Interact* 1998;111–112:277–305.
38. Novo E, Marra F, Zamara E, Valfre di Bonzo L, Monitillo L, Cannito S, et al. Overexpression of Bcl-2 by activated human hepatic stellate cells: resistance to apoptosis as a mechanism of progressive hepatic fibrogenesis in humans. *Gut* 2006;55:1174–1182. [PubMed: 16423888]
39. Parola M, Robino G. Oxidative stress-related molecules and liver fibrosis. *J Hepatol* 2001;35:297–306. [PubMed: 11580156]
40. Sanyal AJ. Mechanisms of disease: pathogenesis of nonalcoholic fatty liver disease. *Nat Clin Pract Gastroenterol Hepatol* 2005;2:46–53. [PubMed: 16265100]
41. Arteel GE. Oxidants and antioxidants in alcohol-induced liver disease. *Gastroenterology* 2003;124:778–790. [PubMed: 12612915]
42. Bataller R, Brenner DA. Liver fibrosis. *J Clin Invest* 2005;115:209–218. [PubMed: 15690074]
43. Thirunavukkarasu C, Watkins S, Harvey SA, Gandhi CR. Superoxide-induced apoptosis of activated rat hepatic stellate cells. *J Hepatol* 2004;41:567–575. [PubMed: 15464236]
44. Montiel-Duarte C, Ansorena E, Lopez-Zabalza MJ, Cenarruzabeitia E, Iraburu MJ. Role of reactive oxygen species, glutathione and NF-kappaB in apoptosis induced by 3,4-methylenedioxymethamphetamine (“Ecstasy”) on hepatic stellate cells. *Biochem Pharmacol* 2004;67:1025–1033. [PubMed: 15006539]
45. Lee KS, Buck M, Houglum K, Chojkier M. Activation of hepatic stellate cells by TGF alpha and collagen type I is mediated by oxidative stress through c-myc expression. *J Clin Invest* 1995;96:2461–2468. [PubMed: 7593635]

46. Dimmeler S, Zeiher AM. Nitric oxide-an endothelial cell survival factor. *Cell Death Differ* 1999;6:964–968. [PubMed: 10556973]
47. Brune B, von Knethen A, Sandau KB. Nitric oxide (NO): an effector of apoptosis. *Cell Death Differ* 1999;6:969–975. [PubMed: 10556974]
48. Beltran B, Quintero V, Garcia-Zaragoza E, O'Connor E, Esplugues JV, Moncada S. Inhibition of mitochondrial respiration by endogenous nitric oxide: a critical step in Fas signaling. *Proc Natl Acad Sci U S A* 2002;99:8892–8897. [PubMed: 12077295]
49. Kurz T, Gustafsson B, Brunk UT. Intralysosomal iron chelation protects against oxidative stress-induced cellular damage. *FEBS J* 2006;273:3106–3117. [PubMed: 16762036]
50. Tenopoulou M, Doulias PT, Barbouti A, Brunk U, Galaris D. Role of compartmentalized redox-active iron in hydrogen peroxide-induced DNA damage and apoptosis. *Biochem J* 2005;387:703–710. [PubMed: 15579135]
51. Cable H, Lloyd JB. Cellular uptake and release of two contrasting iron chelators. *J Pharm Pharmacol* 1999;51:131–134. [PubMed: 10217310]
52. Green DR, Kroemer G. The pathophysiology of mitochondrial cell death. *Science* 2004;305:626–629. [PubMed: 15286356]
53. Modjtahedi N, Giordanetto F, Madeo F, Kroemer G. Apoptosis-inducing factor: vital and lethal. *Trends Cell Biol* 2006;16:264–272. [PubMed: 16621561]
54. DeLeve LD, Wang X, Kanel GC, Ito Y, Bethea NW, McCuskey MK, et al. Decreased hepatic nitric oxide production contributes to the development of rat sinusoidal obstruction syndrome. *Hepatology* 2003;38:900–908. [PubMed: 14512877]
55. Fiorucci S, Antonelli E, Morelli O, Mencarelli A, Casini A, Mello T, et al. NCX-1000, a NO-releasing derivative of ursodeoxycholic acid, selectively delivers NO to the liver and protects against development of portal hypertension. *Proc Natl Acad Sci U S A* 2001;98:8897–8902. [PubMed: 11447266]
56. Moal F, Veal N, Vuillemin E, Barriere E, Wang J, Fizanne L, et al. Hemodynamic and antifibrotic effects of a selective liver nitric oxide donor V-PYRRO/NO in bile duct ligated rats. *World J Gastroenterol* 2006;12:6639–6645. [PubMed: 17075977]
57. Bivalacqua TJ, Champion HC, De Witt BJ, Saavedra JE, Hrabie JA, Keefer LK, et al. Analysis of vasodilator responses to novel nitric oxide donors in the hindquarters vascular bed of the cat. *J Cardiovasc Pharmacol* 2001;38:120–129. [PubMed: 11444495]
58. Feelisch M. The use of nitric oxide donors in pharmacological studies. *Naunyn Schmiedebergs Arch Pharmacol* 1998;358:113–122. [PubMed: 9721012]

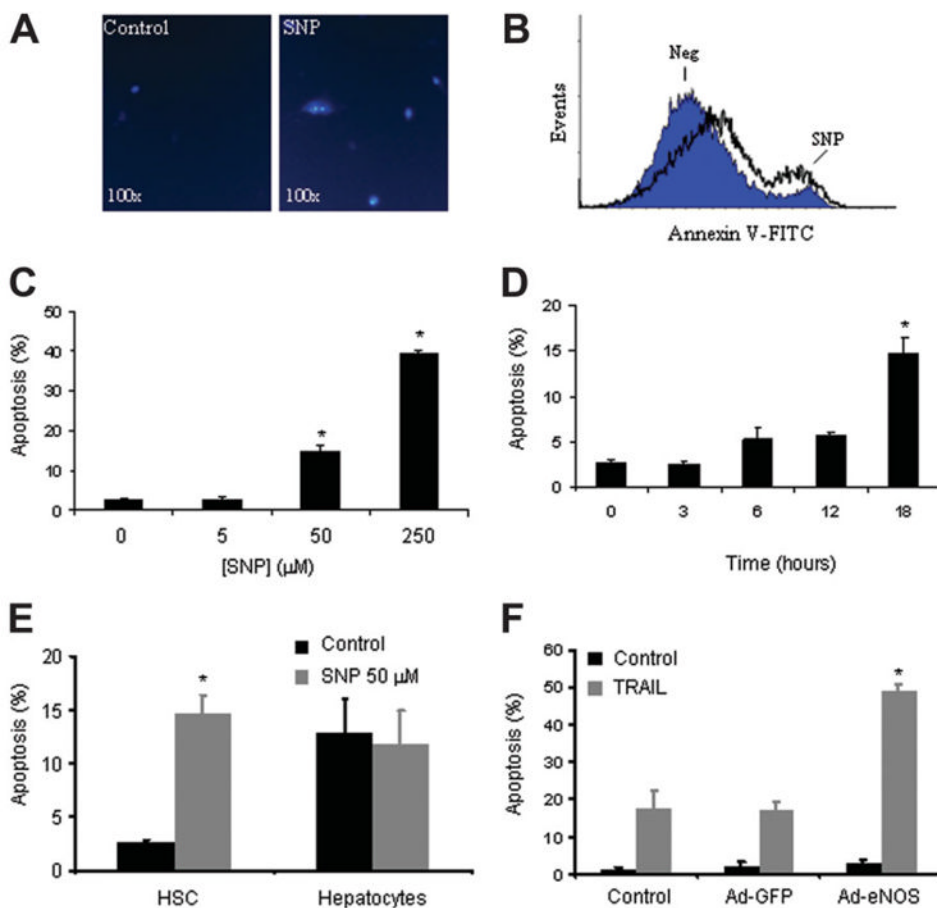


Fig. 1. NO promotes HSC apoptosis

(A) Representative photomicrograph of primary rat HSCs visualized after exposure to NO donor, SNP 50 μM for 18 hours. Cells displayed characteristic chromatin condensation consistent with an apoptotic phenotype by fluorescent microscopy after staining with DAPI 5 $\mu\text{g}/\text{mL}$. (B) Rat HSCs displayed increased annexin-V positivity by flow cytometry after exposure to NO donor SNP 50 μM for 3 hours. (C) Rat HSCs were exposed to increasing concentrations of SNP for 18 hours. Apoptosis was quantitated via DAPI and fluorescent microscopy; HSC apoptosis was concentration-dependent (0 to 250 μM). * $P < 0.01$ compared with all other groups ($n = 10$). (D) Rat HSCs were exposed to 50 μM SNP for increasing time intervals. Apoptosis was quantitated via DAPI and fluorescent microscopy; HSC apoptosis was time-dependent. * $P < 0.05$ compared with all other groups ($n = 3$). (E) Primary rat HSCs and hepatocytes were exposed to 50 μM SNP for 18 hours, and apoptosis was quantitated. Unlike HSCs, hepatocyte apoptosis was not influenced by SNP. * $P < 0.05$ compared with control HSCs ($n = 3$). (F) Human HSC line LX2 was adenovirally transduced with green fluorescent protein, eNOS, or no virus followed by exposure to death receptor agonist TRAIL (10 ng/mL). Cells overexpressing eNOS were significantly more sensitive to death receptor-mediated apoptotic signaling. * $P < 0.01$ compared with green fluorescent protein plus TRAIL and control plus TRAIL ($n = 3$).

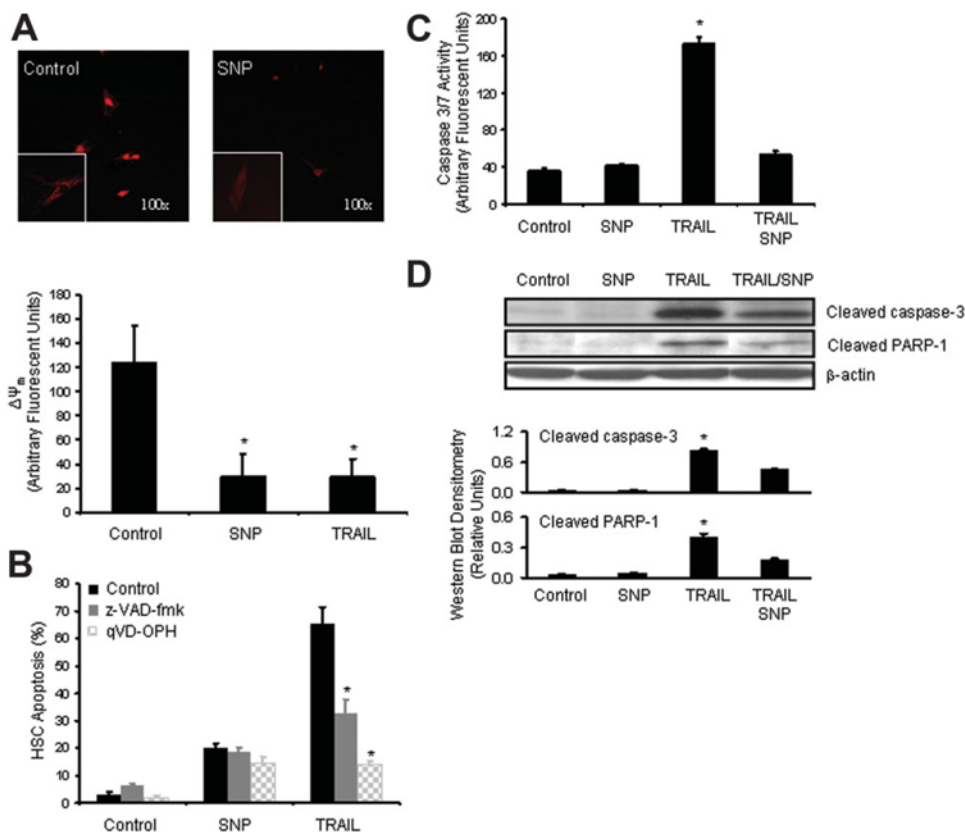


Fig. 2. NO donor-mediated apoptosis is associated with mitochondrial dysfunction and is caspase-independent

(A) HSCs were incubated with SNP for 18 hours and mitochondrial membrane potential ($\Delta\Psi_m$) was determined as described in Materials and Methods. SNP resulted in significant mitochondrial membrane depolarization in HSCs. TRAIL pathway activation (10 ng/mL plus cycloheximide; 3 μ g/mL) served as a positive control (bottom graph). * $P < 0.05$ compared with control ($n = 15$). Representative low magnification micrograph of a cell in response to SNP versus control is depicted [inset: higher magnification (400 \times)]. (B) HSCs were preincubated with pancaspase inhibitors z-VAD-fmk (50 μ M) and qVD-OPH (20 μ M) followed by SNP or vehicle control for 18 hours. Pancaspase inhibition did not impair SNP-mediated apoptosis but did significantly blunt apoptosis in response to TRAIL (10 ng/mL plus cycloheximide 3 μ g/mL) death receptor positive control. * $P < 0.05$ compared with TRAIL receptor stimulation ($n = 6$). (C) Caspase 3 and 7 activity was quantitated from HSCs after exposure to indicated reagents for 18 hours as described in Materials and Methods. There was no increase in effector caspase activity upon exposure to NO donor SNP. Furthermore, SNP abrogated caspase activity induced by TRAIL death receptor stimulation. * $P < 0.05$ compared with all other groups ($n = 3$). (D) Western blot analysis for cleaved caspase 3 and downstream effector PARP-1 demonstrate lack of SNP-induced activation of caspase or PARP-1 cleavage in HSCs (representative western blotted membrane and densitometric quantitation are shown). Cleaved products indicated activation of proenzymes.

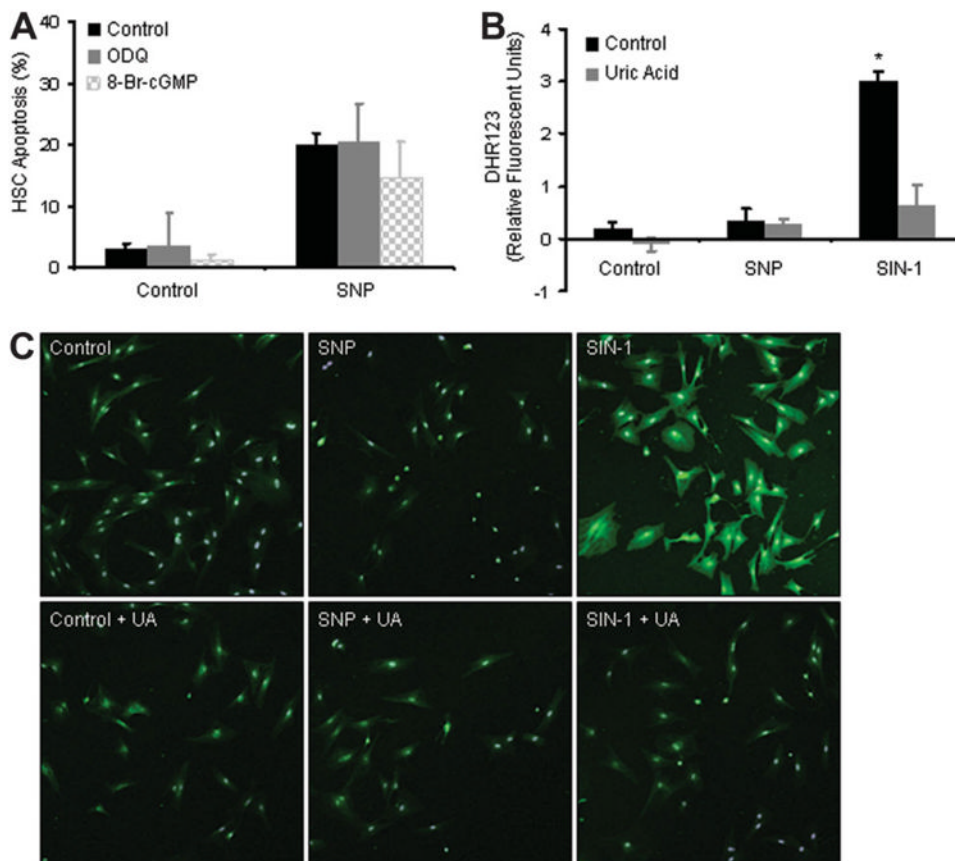


Fig. 3. SNP-mediated apoptosis does not require soluble guanylate cyclase or protein nitration (A) HSCs were preincubated with the cGMP mimetic, 8-Br-cGMP, or guanylate cyclase antagonist, ODQ (100 μ M), followed by exposure to SNP for 18 hours. SNP-mediated apoptosis was not significantly changed by 8-Br-cGMP or ODQ. (B) HSCs were incubated with SNP or the peroxynitrite donor SIN-1 as a positive control for 3 hours in the presence or absence of uric acid (1 mM), a peroxynitrite scavenger. Peroxynitrite generation was measured using the specific fluorescent probe, DHR123. Unlike SIN-1, SNP did not stimulate peroxynitrite generation. * $P < 0.05$ compared with all other groups ($n = 3$). (C) HSCs were exposed to SNP or SIN-1 in the presence or absence of uric acid (1 mM) for 3 hours and then prepared for immunofluorescence microscopy using an antibody that recognizes nitrated tyrosine residues. SIN-1 promoted pancellular protein nitration that was blocked by uric acid, whereas SNP did not promote protein nitration.

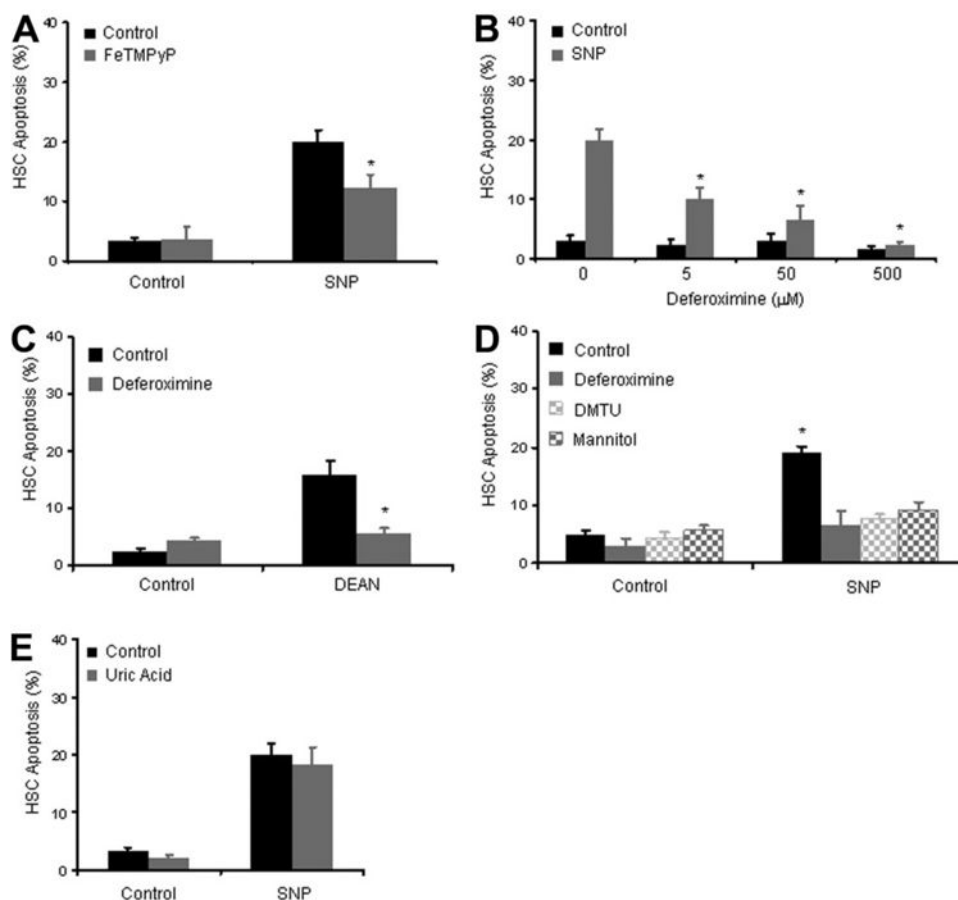


Fig. 4. SNP stimulation of apoptosis is dependent on generation of oxidative stress

(A) HSCs were preincubated with the SOD mimetic FeTMPyP, then stimulated with SNP and analyzed for apoptosis after 18 hours. FeTMPyP significantly inhibited SNP induced apoptosis by 40%. $*P < 0.05$, FeTMPyP compared with FeTMPyP plus SNP ($n = 3$). (B) HSCs were preincubated with varying concentrations of hydroxyl ion scavengers deferoxamine, and apoptosis was determined in response to SNP (50 μM). Deferoxamine attenuated SNP-induced apoptosis in a concentration-dependent manner with complete abrogation of apoptosis at the highest concentration of deferoxamine. $*P < 0.05$ compared with SNP 50 μM in the absence of deferoxamine ($n = 3$). (C) Deferoxamine also attenuated apoptosis induced by an alternative NO donor, DEAN. $*P < 0.05$ compared with 1 mM DEAN in the absence of deferoxamine ($n = 3$). (D) HSCs were preincubated with hydroxyl ion scavengers deferoxamine, mannitol (50 μM), or dimethylthiourea (50 μM), and apoptosis was determined in response to SNP (50 μM). Similar to deferoxamine, both mannitol and dimethylthiourea inhibited SNP-induced apoptosis of HSCs. $*P < 0.05$ compared with SNP 50 μM ($n = 3$). (E) HSCs were preincubated with the peroxynitrite scavenger uric acid (1 mM) followed by incubation with SNP. Uric acid did not influence SNP-mediated apoptosis.

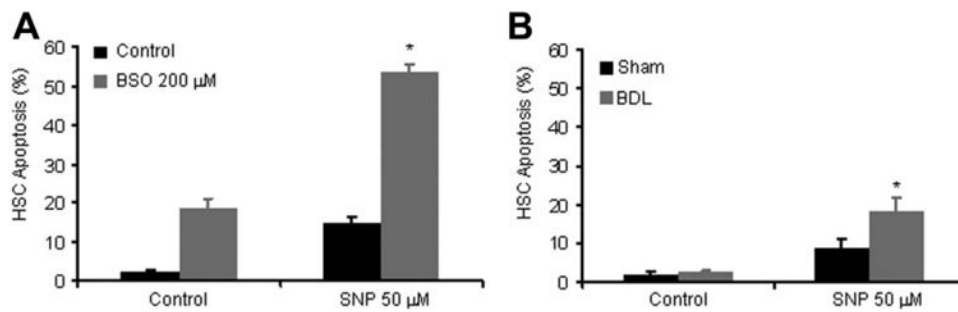


Fig. 5. Oxidative stress exacerbates SNP-dependent apoptosis

(A) HSCs were preincubated with the glutathione-depleting agent, BSO, then exposed to SNP or vehicle, and analyzed for apoptosis. BSO sensitized HSCs to SNP-mediated apoptosis. $*P < 0.05$ compared with all other groups ($n = 3$). (B) HSCs were isolated and cultured from BDL and sham-operated rats. Cells were exposed to SNP or vehicle and then analyzed for apoptosis after 18 hours. HSCs isolated from BDL rats were significantly more susceptible to SNP-mediated apoptosis compared with HSCs isolated from sham-operated rats. $*P < 0.05$ compared with all other groups ($n = 3$).